Received: 6 October 2023 | Accepted: 9 February 2024

DOI: 10.1111/ppl.14227

ORIGINAL RESEARCH

Physiologia Plantarum

Transcriptomic and proteomic analyses of distinct Arabidopsis organs reveal high PSI-NDH complex accumulation in stems

Laura Laihonen | Marjaana Rantala | Umanga Ranasinghe | Esa Tyystjärvi | Paula Mulo

Molecular Plant Biology, Department of Life Technologies, University of Turku, Turku, Finland

Correspondence
Paula Mulo,
Email: pmulo@utu.fi

Esa Tyystjärvi,
Email: esatyy@utu.fi.

Funding information
Research Council of Finland, Grant/Award Numbers: 321616, 333421; Suomen Kulttuurirahasto, Grant/Award Numbers: 00220578, 00230972

Edited by W. Schröder

Abstract

In addition to leaves, the main site of photosynthetic reactions, active photosynthesis also takes place in stems, siliques and tree trunks. Although non-foliar photosynthesis has a marked effect on plant growth and yield, only limited information on the expression patterns of photosynthesis-related genes and the structure of photosynthetic machinery in different plant organs has been available. Here, we report the results of transcriptomic analysis of various organs of *Arabidopsis thaliana* and compare the gene expression profiles of young and mature leaves with a special focus on photosynthetic genes. Further, we analyzed the composition and organization of the photosynthetic electron transfer machinery in leaves, stems and green siliques at the protein level using BN-PAGE. RNA-Seq analysis revealed unique gene expression profiles in different plant organs and showed major differences in the expression of photosynthesis-related genes in young as compared to mature rosettes. Gel-based proteomic analysis of the thylakoid protein complex organization further showed that all studied plant organs contain the necessary components of the photosynthetic electron transfer chain. Intriguingly, stems accumulate high amounts of PSI-NDH complex, which has previously been implicated in cyclic electron transfer.

1 | INTRODUCTION

Plants are primary producers that are able to harvest and convert solar energy into chemical form through photosynthesis. Photosynthesis, as well as various other reactions, such as biosynthesis of lipids, pigments and hormones, take place in chloroplasts, which are semi-autonomous cell organelles surrounded by an inner and outer envelope membrane. The envelope membrane encloses thylakoid membranes, which embed the pigment-protein complexes catalyzing the photosynthetic electron transfer reactions. Photosynthetic electron transfer results in the production of NADPH and ATP, which are used in downstream metabolism, most importantly in carbon assimilation. Carbon assimilation is followed by the generation of various kinds of carbon compounds, which fuel all heterotrophic life on Earth.

In linear electron transfer chain (LET), electrons from water are transferred from photosystem II (PSII) to photosystem I (PSI) via cytochrome (Cyt) b_6f and two mobile electron carriers, plastoquinone (PQ) and plastocyanin (PC), eventually producing reducing equivalents of NADPH. During the electron flow, a proton gradient across the thylakoid membrane is generated, which then empowers the production of ATP through ATPase. The cyclic electron transfer (CET) chain, in turn, cycles electrons around PSI and produces only ATP (Shikanai, 2007). Although the molecular mechanisms and functional significance of CET are not fully understood, CET is known to take

place through at least two pathways. The antimycin A sensitive pathway depends on PROTON GRADIENT REGULATION (PGR5) and PGRL1 proteins, while the antimycin A insensitive route depends on the NADH dehydrogenase (NDH) complex (Johnson, 2011; Shikanai, 2007). CET is considered to be important for balancing ATP and NADPH production, but it is also crucial in regulation of LET, as increased proton gradient across the membrane slows down electron flow through Cyt b_6f (photosynthetic control) and activates non-photochemical quenching (NPQ), which safely dissipates excess excitation as heat. These mechanisms protect PSI and PSII from photodamage (Aro et al., 1993; Johnson, 2011; Munekage et al., 2004; Müller et al., 2001; Tiwari et al., 2016).

The vast majority of studies concerning photosynthesis have been carried out on leaves, whereas other green tissues have been widely overlooked. Nevertheless, for instance, stems, siliques and tree trunks have been shown to have the capability to perform photosynthesis (Hibberd & Quick, 2002; Saveyn et al., 2010; Sun et al., 2021; Xu et al., 1997) and non-foliar photosynthesis has been implicated to have a marked effect on plant growth and yield (Simkin et al., 2020). Additionally, photosynthesis in non-foliar tissues has been shown to contribute to abiotic stress tolerance (Kong et al., 2010; Sánchez-Díaz et al., 2002), and especially stem photosynthesis appeared to be a significant carbon source for the plants in the Mediterranean climate characterized by hot and dry summers (Yiotis et al., 2008). Leaves, green stems, and green flower organs are optimized for harvesting atmospheric CO_2, which enters the cell through stomata. In contrast, other tissues in which atmospheric CO_2 cannot penetrate (e.g. tree trunks) rely either on respiration as the major carbon source or on the transportation of carbon through the vascular system (Henry et al., 2020; Hibberd & Quick, 2002).

In addition to the tissue type and cellular environment of the chloroplast, age has an additional impact on the photosynthetic reactions and chloroplast metabolism in general (Baumgartner et al., 1989; Munné-Bosch & Alegre, 2002). For instance, transcriptional activity in the plastids of young cells of barley leaves is increased (Baumgartner et al., 1989), and there is a higher accumulation of *rbcL* mRNA in young leaves of Arabidopsis compared to older ones (Zoschke et al., 2007). Despite the importance of non-foliar photosynthesis and obvious age-dependent changes in chloroplast metabolism, gene expression patterns with a focus on photosynthetic genes and composition of the photosynthetic machinery in distinct Arabidopsis organs and at various developmental stages have remained unstudied.

Here, we examined the gene expression profiles of different organs of *Arabidopsis thaliana*, paying special attention to the expression of photosynthetic genes, and studied the organization of chloroplast-located photosynthetic electron transfer machinery in different plant organs using gel-based proteomic methods. Moreover, we compared the gene-expression profiles of young and mature rosettes to highlight the importance of selecting plants in the appropriate developmental stage for various (omics) analyses. Furthermore, the gel-based proteomic analysis demonstrated that plant stems and siliques contain all the components of the photosynthetic electron transfer chain, but intriguingly, stems accumulate high amounts of CET-related PSI-NDH complex.

2 | MATERIALS AND METHODS

2.1 | Plant growth

Arabidopsis thaliana Col-0 plants were grown on a peat: vermiculite mixture (2:1) in 8/16 h light/darkness for short day conditions for five weeks (mature rosette, MR) or three weeks (young rosette, YR), and in 16/8 h light/ darkness (stems, flowers, green siliques) for 6 weeks at photosynthetic photon flux density (PPFD) of 120 µmol m^{-2} s^{-1} (Osram Powerstar HQI®-BT 400 W/D PRO Daylight), 50% humidity at 23°C. Different biological replicates were grown on separate trays at different times. For the production of root material, surface sterilized seeds were plated on half-strength Murashige and Skoog (Duchefa) plates with 0.8% plant agar. The plants were grown under the light rhythm of 8 /16 h light/darkness at PPFD of 50 µmol m^{-2} s^{-1}, 50% humidity, and 23°C in a vertical position in an incubator for six weeks. Four biological replicates were used in the RNA-Seq analysis, and three biological replicates were used in the gel-based proteomic analyses.

2.2 | RNA isolation

RNA was extracted from 100 mg of each plant material using the innuPREP Plant RNA kit (Analytik Jena) according to the manufacturer's protocol. Lysis Solution RL was used for young and mature rosettes, flowers and roots, while lysis solution PL was used for stems. DNase treatment was done with the TURBO DNA-free Kit (Thermo Fisher Scientific), and concentration was measured using a DeNovix DS-11 series spectrophotometer (DeNovix Inc.). After removal of DNA, RNA quality and integrity were assessed on 1% agarose gel.

2.3 | RNA-Seq analysis and determination of differentially expressed genes

RNA (500 ng) from each plant material was provided to the Finnish Functional Genomics Center (Turku) for PolyA+ transcriptome sequencing (RUO). The quality of the samples was ensured using Agilent Bioanalyzer 2100 or Advanced Analytical Fragment Analyzer. Sample concentration was measured with Qubit®/Quant-IT® Fluorometric Quantitation (Life Technologies) and/or KAPA Library Quantification kit for Illumina platform (KAPA Biosystems). The paired-end libraries were sequenced using the Illumina NovaSeq 6000 S1 v1.5 (Illumina) as 50 bp paired-end reads with an average quality score (Q30) of above 90%.

Chipster v. 4 (Kallio et al., 2011) was used for data analysis (http://chipster.csc.fi/). Reads were mapped to the Arabidopsis genome TAIR10.42 with Bowtie2 (Langmead and Salzberg 2012).

The number of alignments mapped to each gene was counted using HTseq2 (Putri et al., 2022).

Differential expression analysis was done with the DESeq2 package (Love et al., 2014) using the Chipster platform (Kallio et al., 2011). Differentially expressed genes were filtered by using the absolute value of the log2 fold-change of 1 and FDR-value <0.05 as thresholds. Heatmaps were generated using the online available tool https://build.ngchm.net/NGCHM-web-builder, NG-CHM BUILDER. Venn diagrams were made with a web-based tool (https://bioinformatics.psb.ugent.be/webtools/Venn/). GO analysis for DEGs was made with Gene Ontology Term Enrichment for Plants in TAIR with biological function or cellular compartment as GO aspects. RNA-Seq data are available in GEO (accession GSE233562).

2.4 | Isolation of thylakoid membranes

Each plant material was collected in ice-cold grinding buffer [50 mM Hepes/KOH (pH 7.5), 330 mM sorbitol, 5 mM MgCl2, 5 mM sodium-L-ascorbate and 0.1% BSA, 10 mM sodium fluoride], and the suspension was filtered through Miracloth followed by centrifugation at 2739 g at 4°C for 5 min. The pellet was resuspended in shock buffer [50 mM Hepes/KOH (pH 7.5), 5 mM MgCl2, 10 mM sodium fluoride] and centrifuged at 2739 g at 4°C for 5 min. The pellet was washed with storage buffer [50 mM Hepes/KOH (pH 7.5), 100 mM sorbitol, 5 mM MgCl2,10 mM sodium fluoride] followed by centrifugation at 2739 g at 4°C for 5 min. Finally, the pellet was resuspended in storage buffer. Chlorophyll concentration was determined from the samples according to (Porra et al., 1989).

2.5 | SDS-PAGE and Western blotting

Isolated thylakoids were solubilized with Laemmli buffer (138 mM Tris–HCl pH 6.8; 6 M Urea, 22.2% (v/v), 4.4% SDS) containing 10% β-mercaptoethanol. The sample was loaded on SDS-gel (12% acrylamide, 6 M urea) on chlorophyll basis as follows: 0.5 μg of Chl for Phospho-Thr/Ser antibody (Cell Signaling Technology, 9381S; 1:6000) and 1 μg of Chl for D1 (DE-loop antibody (Kettunen et al., 1996); 1:8000), PSAB (AS10695; 1:2500, Agrisera), ATPB (AS05085; 1:5000, Agrisera) and Cyt f (AS06119; 1:1000, Agrisera), and 4 μg Chl for NDHL (T. Shikanai; 1:5000) and LHCA5 (AS05082; 1:3000, Agrisera). The proteins were electroblotted onto Immobilon-FL membrane (Merck Millipore), blocked with 5% milk or bovine serum albumin (BSA) in TTBS (20 mM Tris–HCl, pH 7.5, 150 mM NaCl, and 0.05% Tween 20) and incubated with primary antibody overnight. The membrane was incubated with a secondary antibody, either IRDye® 800CW Goat anti-Rabbit IgG (1:20 000 in 1% milk/TTBS) for Li-Cor Odyssey or with ECL Anti-rabbit IgG HRP (1:10 000 in 1% milk/TTBS, NA9340V, GE Healthcare). After incubation, the membrane was imaged with Li-Cor Odyssey CLx or incubated for 5 min in ECL (Amersham) and developed on Super RX-N x-ray films (Fujifilm).

2.6 | BN-PAGE and 2D-BN-SDS-PAGE

Thylakoid samples were diluted in BTH buffer [25 mM BisTris/HCl (pH 7.0), 20% (w/v) glycerol and 0.25 mg ml^{-1} Pefa- bloc, 10 mM NaF]. An equal volume of 2% beta-dodecylmaltoside (β-DDM) (Sigma-Aldrich) in BTH buffer was added to the sample to achieve a final concentration of 0.5 mg ml^{-1} of Chl and 1% β-DDM in the sample and incubated on ice for 2 min. The membrane debris was pelleted by centrifugation at 18 000 g at 4°C for 25 min and the soluble protein complexes were used for the analysis. The solubilized thylakoid protein complexes were separated with BN-PAGE (3,5–12.5% acrylamide) as described by Järvi et al. (2011). 7 μg of Chl of each sample was loaded on the gel. The 2D-BN-SDS-PAGE (12% acrylamide, 6 M Urea) was performed as described by Järvi et al. (2011), followed by silver staining according to Blum et al. (1987). Five protein spots were cut from the 2D-BN-SDS gel and digested according to the standard protocol for identification with LC-ESI-MS/MS analysis.

2.7 | LC-ESI-MS/MS Analysis

The digested peptide samples were dissolved in 15 μL of 0.1% formic acid, and 5 μL of each gel sample was analyzed. The LC-ESI-MS/MS analyses were performed on a nanoflow HPLC system (Easy-nLC1000, Thermo Fisher Scientific) coupled to the Q Exactive HF mass spectrometer (Thermo Fisher Scientific) equipped with a nano-electrospray ionization source. Peptides were first loaded on a trapping column and subsequently separated on a 15 cm C18 column (75 μm × 15 cm, ReproSil-Pur 3 μm 120 Å C18-AQ, Dr. Maisch HPLC GmbH, Ammerbuch-Entringen). The mobile phase consisted of water with 0.1% formic acid (solvent A) or acetonitrile/water (80:20 (v/v)) with 0.1% formic acid (solvent B). A 20 min gradient was used to elute peptides (10 min from 8 to 43% of solvent B and 5 min from 43 to 100% of solvent B, followed by a 5 min wash stage with solvent B). MS data was acquired automatically by using Thermo Xcalibur 4.1 software (Thermo Fisher Scientific). The information dependent acquisition method consisted of an Orbitrap MS survey scan of mass range 300–2000 m/z followed by HCD fragmentation for the ten most intense peptide ions.

3 | RESULTS

3.1 | Gene expression analysis of young and mature rosettes

To explore the differences in transcriptomes of 3-week-old (young) and 5-week-old (mature) Arabidopsis rosettes composed of leaves in different developmental stages, total RNA was isolated, and nuclear mRNA was sequenced using the Illumina platform. A total of ~19 000 expressed genes, using an average of 10 reads/biological replicate as a threshold, were identified in both young and mature rosettes (Figure 1A). Although the vast majority of the detected transcripts

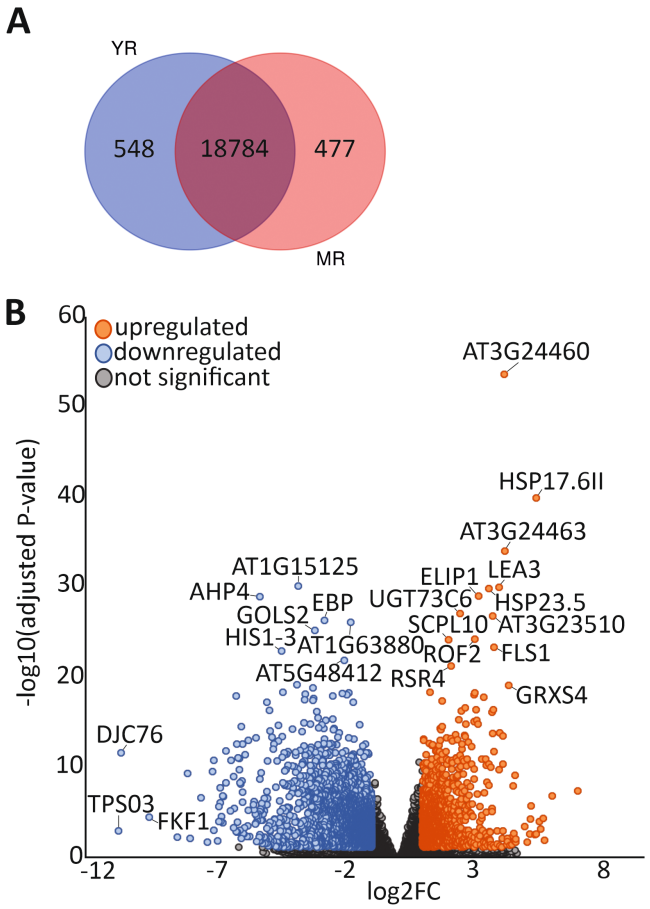

FIGURE 1 **Gene expression analysis of mature and young Arabidopsis rosettes. (A)** Venn diagram showing commonly and uniquely expressed genes in young and mature rosettes. For comparison of the transcriptome of different aged rosettes, total RNA was isolated from four biological replicates of 3-week old rosettes (YR) and 5-week old mature rosettes (MR) followed by RNA sequencing by Illumina platform. Expressed genes in each sample type were chosen from RNA-Seq data using an average of 10 reads/one biological replicate as a threshold for expressed genes. (**B**) Volcano plot of differentially expressed genes (DEGs) in young versus mature rosettes. Horizontal axis shows log2fold-change value, whereas vertical axis shows the level of significance with adjusted p-value. |Log2fold-change| >1 and adjusted P-value of <0.05 were used as thresholds for significantly up- or downregulated genes.

were identified in both young and mature rosettes, both expressed around 500 unique genes (Figure 1A).

Pairwise analysis of differentially expressed genes (DEGs) revealed significant differences in the expression levels in the mutually expressed genes of the young and mature rosettes (Figure 1B, Dataset S1). GO enrichment analysis of the biological function of DEGs indicated that many of the upregulated genes in young rosettes were involved in photosynthesis-related processes (responses to light quality or quantity, 'chlorophyll metabolic process' and 'pigment biosynthesis process') (Figure 2A, Datasets S2 and S3), while the majority of the downregulated genes were assigned to biological processes related to biotic stress responses. Further details and categorization of the DEGs are listed in supplementary datasets S2 and S3.

In order to better understand how leaf age affects the expression of genes involved in photosynthetic reactions, photosynthesis-related genes were manually filtered from the gene list after conducting differential expression analysis with DESeq2 (Love et al., 2014) within Chipster (Kallio et al., 2011), and a heatmap was generated using NG-CHM Builder (Figure 2B, Dataset S4). Selected genes were assigned to four categories: (1) Photosystem II (PSII) and light harvesting complex II (LHCII)-associated genes, (2) Photosystem I (PSI) and light harvesting complex I (LHCI)-associated genes, (3) Calvin-Benson-Bassham (CBB) cycle-associated genes and (4) Other, such as genes encoding components of ATP- and NDH-complexes, or regulatory proteins. In young rosettes, the majority of DEGs related to the photosynthetic light reactions (classes 1 and 2) were slightly upregulated as compared to those of mature rosettes, but the changes were not statistically significant (Figure 2B). However, expression of some genes encoding subunits of the PS and LHC complexes, namely *PSBQ-1*, *LHCB7*, *LHCA5*, *LHCA6*, *PSAF* and *PSAH1* genes were significantly upregulated, while *PSBQ-2* was downregulated in young rosettes (Figure 2B). On the contrary, a number of CBB cycle related DEGs (class 3), including genes encoding RuBisCo subunits, were significantly upregulated in young rosettes as compared to mature rosettes. Moreover, many regulatory genes (class 4), such as *STN8*, *PGR5* and genes encoding subunits of NDH-complex and ATP-synthase, were also upregulated in young rosettes.

3.2 | Comparison of organ-specific transcriptomes and expression of photosynthesis related genes

To get an insight into the gene expression patterns of distinct plant organs, total RNA from 5-week-old rosettes and 6-week-old stems, flowers and roots was isolated, followed by RNA-seq library generation and sequencing by Illumina platform. The results are applicable to many laboratories, as the studied plant material was produced under conditions frequently used in research: leaf material in short-day conditions, stems, flowers and siliques in long-day conditions, and root material on agar plates. Around 18 000 transcripts were commonly detected in all plant organs (Figure S1A). The rosettes and stems expressed only ~100 and ~200 unique transcripts, respectively, while in both roots and flowers, ~1000 of the transcripts were unique (Datasets S5, S6 and S7). Pairwise DEG analysis was conducted to investigate the expression levels of the mutually expressed genes by comparing each organ (stems, flowers or roots) to mature rosettes (Figure S1B, Datasets S8, S9 and S10). GO analysis of DEGs revealed that the majority of the upregulated genes in flowers and roots were related to reproduction or root development, respectively, as expected (Datasets S11–S16).

Because knowledge of the expression of genes related to photosynthesis in non-foliar green tissues provides the basis for understanding non-foliar photosynthesis, expression patterns of manually selected photosynthesis-related DEGs were analyzed (Dataset S4). Results for roots are shown for comparison. In general, the majority of photosynthetic genes are downregulated in flowers, roots and stems

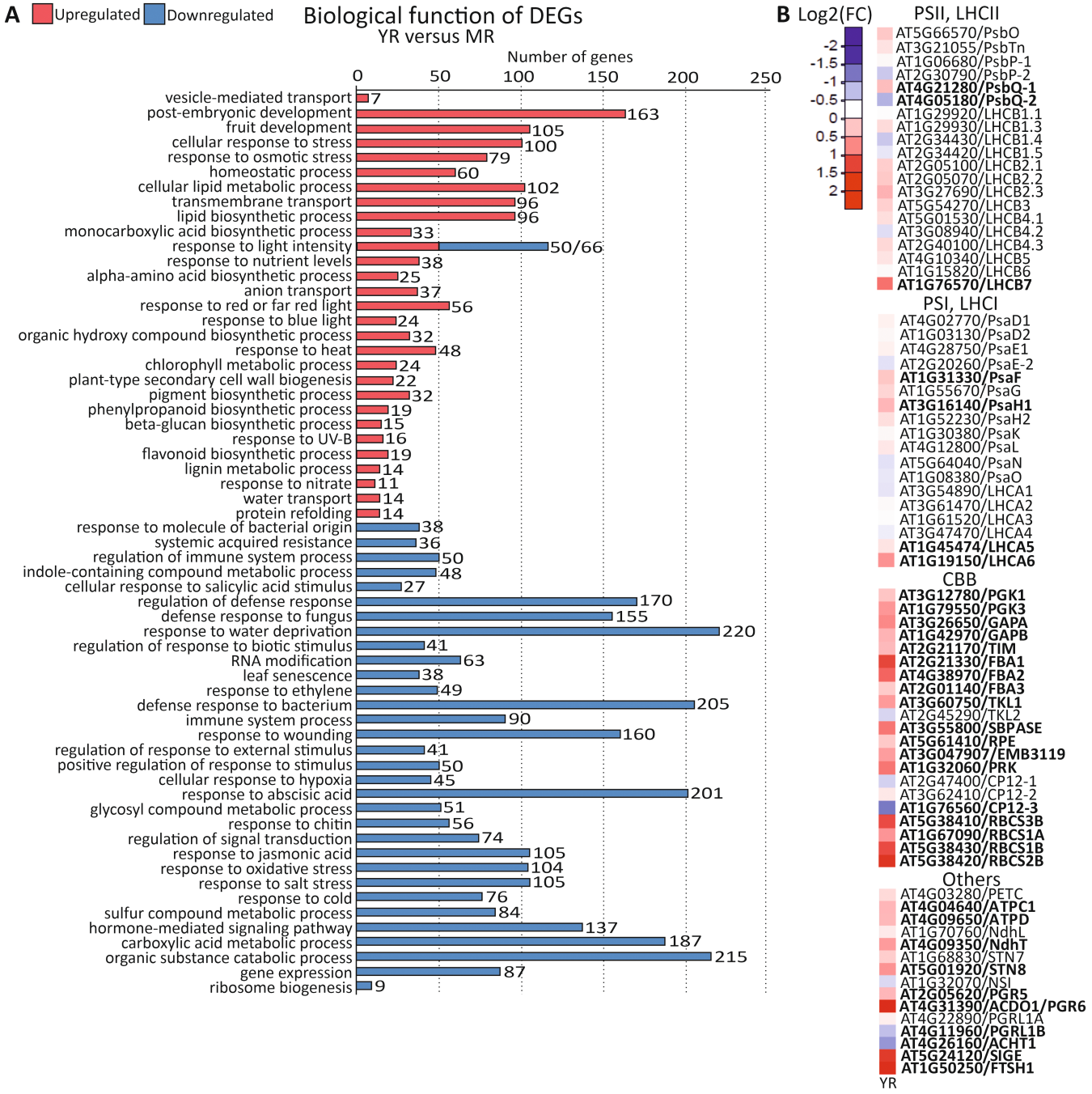

FIGURE 2 **Expression analysis of photosynthesis-related genes in young and mature rosettes. (A)** Gene ontology (GO) classification of biological function of differentially expressed genes (DEGs) in 3-week old young rosette (YR) versus 5-week old mature rosette (MR). DEGs from YR versus MR analysis were filtered using adjusted P-value <0.05 and |Log2fold-change| >1 as thresholds, and GO classification was made based on biological process of DEGs. The amounts of upregulated genes in YR compared to MR in each category are indicated with red bars, whereas downregulated with blue bars. The number of genes allocated to a specific category is presented after the bar. (**B**) The relative expression patterns of differentially expressed genes (DEGs) involved in photosynthesis. DESeq2 analysis was performed with DESeq2 for RNA-Seq-data from 3-week old young rosettes (YR) and 5-week old mature rosettes (MR). MR was used as a control. Photosynthetic genes were chosen from the list manually and divided to four categories: photosystem II (PSII) and light harvesting complex II (LHCII)-associated genes, photosystem I (PSI) and light harvesting complex I (LHCI)-associated genes, Calvin-Benson-Bassham (CBB) cycle-associated genes and others, such as regulatory genes. Upregulated genes are indicated with red color whereas downregulated with blue. Fold-changes are presented as log2fold-changes. Statistical significance is indicated with bolding the gene name.

as compared to leaves (Figure 3). However, *TRANSKETOLASE2* (TKL2, AT2G45290), catalyzing the formation of xylulose 5-phosphate and erythrose 4-phosphate within the regenerative part of the CBB cycle (Villafranca & Axelrod, 1971), was highly upregulated in flowers (6-fold), roots (9-fold) and stems (10-fold) compared to leaves (Figure 4). *CP12-3* (AT1G76560), *ACDO1* (PGR6, AT4G31390),

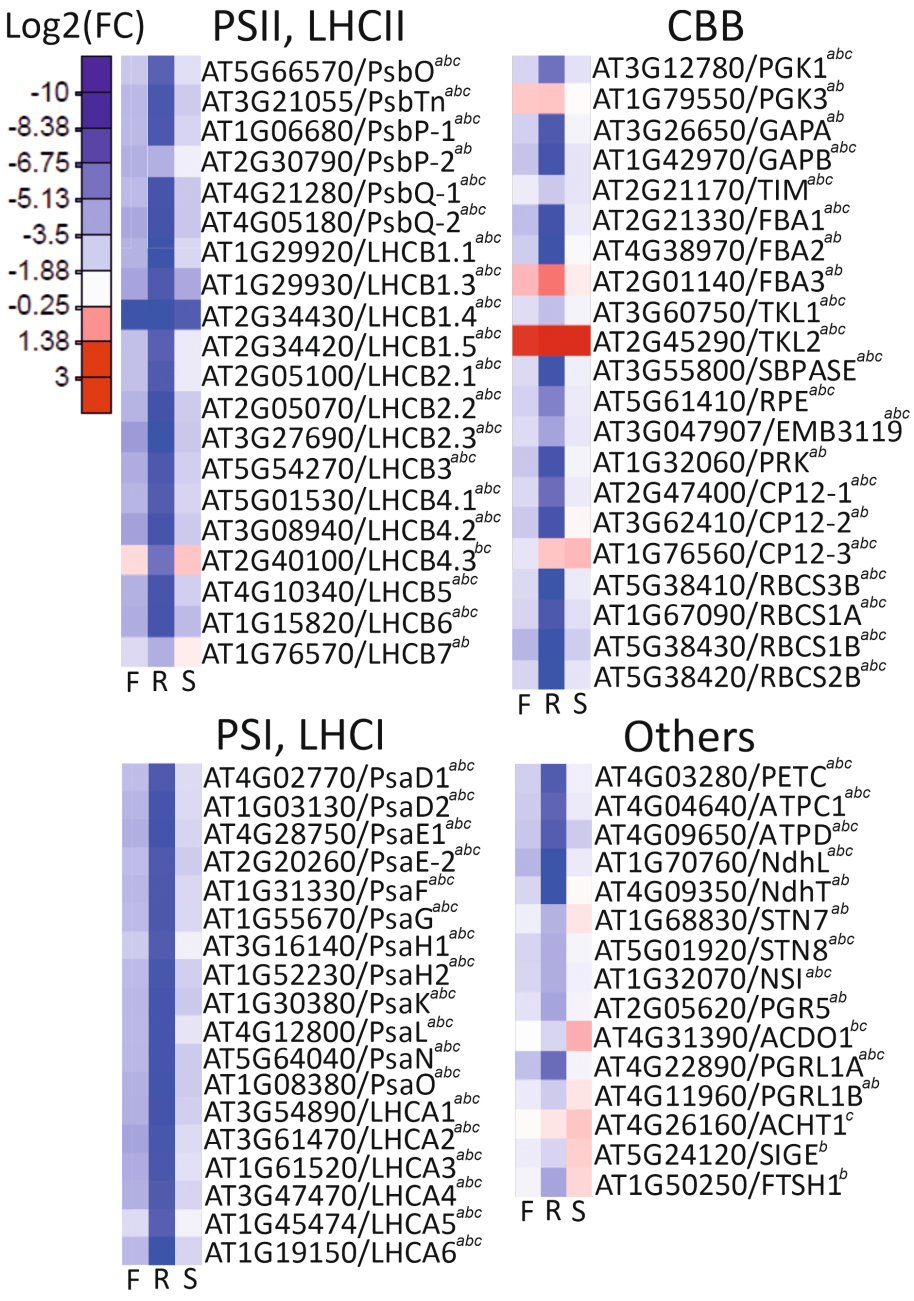

FIGURE 3 **The relative expression patterns of differentially expressed genes (DEGs) involved in photosynthesis.** Differential expression was analyzed with DESeq2 for RNA-Seq-data from flowers (F), roots (R), stems (S) and 5-week old rosettes. Mature rosettes were used as a control. Photosynthetic genes were chosen from the list manually and divided in four categories: photosystem II (PSII) and light harvesting complex II (LHCII)-associated genes, photosystem I (PSI) and light harvesting complex I (LHCI)-associated genes, Calvin-Benson-Bassham (CBB) cycle-associated genes and others, such as regulatory genes. Upregulated genes are indicated with red color whereas downregulated with blue. Fold-changes are presented as log2fold-changes. Statistical significance indicated with *a* (flowers versus rosette), *b* (roots versus rosette) and *c* (stems versus rosette).

LHCB4.3 (AT2G40100) and *ACHT1* (AT4G26160) were significantly upregulated in stems. In flowers, *PGK3* (AT1G79550) and *FBA3* (AT2G01140) were upregulated. *FBA3*, *PGK3* and *CP12-3* were significantly upregulated in roots, whereas nearly all other genes associated with photosynthesis were significantly downregulated in roots as compared to leaves, as expected.

3.3 | Gel-based proteomic analysis of the photosynthetic protein complexes in the thylakoid membrane

Proteomic characterization of the photosynthetic machinery has usually been conducted with leaf material, while very little is known about the composition and organization of photosynthetic machinery in other organs. Most of the genes related to photosynthesis were downregulated in non-foliar organs, including the genes encoding the main components of photosynthetic machinery (Figure 3). Thus, we next studied whether the thylakoid membrane-embedded photosynthetic machinery is qualitatively similar in different plant organs using gel-based proteomic methods. Roots were left out from the proteomic analysis as there are neither chloroplasts nor thylakoid structures in the roots. Flower sepals contain only a few chloroplasts and thus, green siliques were analyzed instead. Thylakoids isolated from mature rosettes, stems, and green siliques of Arabidopsis were solubilized with β-DDM, which solubilizes intact protein complexes from the thylakoid membranes. Solubilized protein complexes were loaded on a chlorophyll basis and separated on BN-PAGE (Figure 4A).

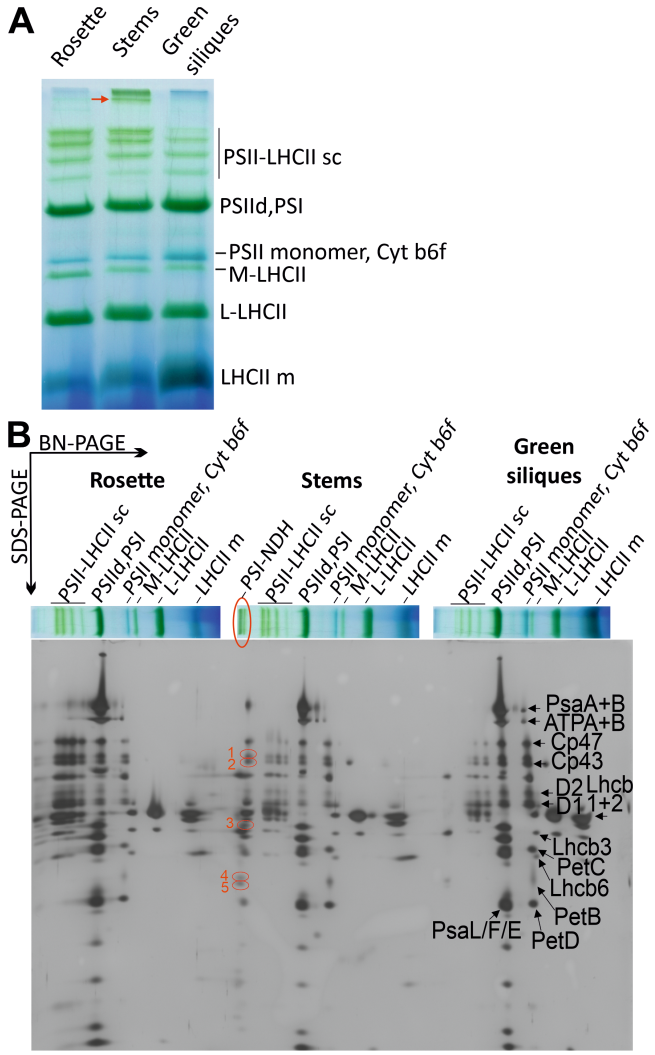

FIGURE 4 **Two-dimensional lpBN/SDS-PAGE analysis of thylakoid proteins of rosettes, stems and green siliques. (A)** Thylakoid proteins were solubilized with beta-dodecylmaltoside (β-DDM) and protein complexes were separated according to their molecular mass with large pore BN-PAGE (lpBN-PAGE). 7 ug of Chl of solubilized protein complexes were loaded on gel. **(B)** Protein subunits were further analyzed by separating them with 2D-BN-SDS-PAGE and silver staining. Identification of protein spots is based on Aro et al. 2005. PSI-NDH is indicated with red circle. Spots analyzed with LC–MS/MS analysis are marked with red circles and numbers 1–5.

Interestingly, the composition and organization of the photosynthetic machinery were qualitatively similar in all studied plant organs (Figure 4A). Indeed, the thylakoid membranes of stems and green siliques contained PSII-LHCII supercomplexes, PSI, Cyt b_6f and ATPase similarly to the leaves, indicating fully functional photosynthetic machinery. Intriguingly, increased amounts of high molecular weight protein complexes (marked with red arrow), that, according to previous studies, represent PSI-NDH complex (Kouril et al., 2014; Aro et al., 2005) co-migrating with PSII-LHCII megacomplexes (Albanese et al., 2016; Aro et al., 2005), were detected in stems (Figure 4A). To confirm the identity of the protein complex, distinct protein subunits were separated on 2D-BN-SDS-PAGE followed by silver staining and LC–MS/MS analysis of specific protein spots (Figure 4B). The MS analysis verified that high number of PSI-NDH subunits (e.g. NDHH, NDHJ, PNSL2, PNSL3, PNSB4, PSAC, PSAD1, PSAE1, PSAE2, PSAF, PSAF, PSAL, LHCA1, LHCA3, LHCA4, LHCA5) as well as subunits of PSII-LHCII (e.g. CP43, CP47) were present in the analyzed protein spots (Figure 4B, Datasets S17–S21). Since the PSI-NDH and PSII-LHCII megacomplexes co-migrate in the same band, it is not possible to determine which complex (or both) accumulates in the stems more than in other studied organs by using 2D-BN-SDS-PAGE analysis. Therefore, we further studied the total accumulation of protein subunits specific for PSI-NDH (NDHL, LHCA5 (Otani et al., 2018; Shimizu et al., 2008)) and PSII-LHCII (D1) in thylakoid samples from immunoblots probed with specific antibodies. A higher accumulation of the NDHL and LHCA5 subunits was detected, while no differences were observed in the accumulation of D1 (Figure 5), suggesting that the PSI-NDH complex accumulates at higher quantities in the thylakoids of stem-localized chloroplasts as compared to those of leaves.

Finally, the accumulation of key subunits of other photosynthetic protein complexes, i.e. PSAB (PSI), Cyt f (Cyt *b6f*) and ATPB (ATPase), were analyzed from immunoblots using specific antibodies (Figure 5). Since phosphorylation of PSII and LHCII proteins is an important regulatory mechanism in plant leaves, the phosphorylation status of PSII core proteins and LHCII was also studied using antibody that recognizes phosphorylated threonine and serine residues. In accordance with the 2D-BN-SDS-PAGE analysis (Figure 4A, B), immunoblots did not reveal any differences in the accumulation of the subunits representing the main photosynthetic complexes between the plant organs (Figure 5). Moreover, the phosphorylation status of the thylakoid proteins in all non-foliar tissues resembled that of the leaves (Figure 5). However, the level of most inspected proteins was slightly lower in siliques as compared to other organs (Figure 5). Furthermore, the overall amount of other protein complexes was more or less similar in all organs, but in green siliques PSII monomers were more abundant than in other organs. Rosettes contained more PSII-LHCII supercomplexes and PSII dimers than stems and siliques (Figure 4B).

4 | DISCUSSION

4.1 | Plant age has a major impact on the expression of photosynthetic genes

Transcriptomes of young and mature rosettes showed striking differences, as ~20% of the commonly expressed genes exhibited statistically significant differential age-dependent expression patterns (Figure 1B). Importantly, our results revealed significant upregulation of various genes involved in photosynthetic carbon assimilation in young as compared to mature rosettes, while the expression of genes coding for the photosystems and light-harvesting complexes were not markedly dependent on plant age (Figure 2B). These results are in line with previous studies showing distinct changes in plant metabolism in

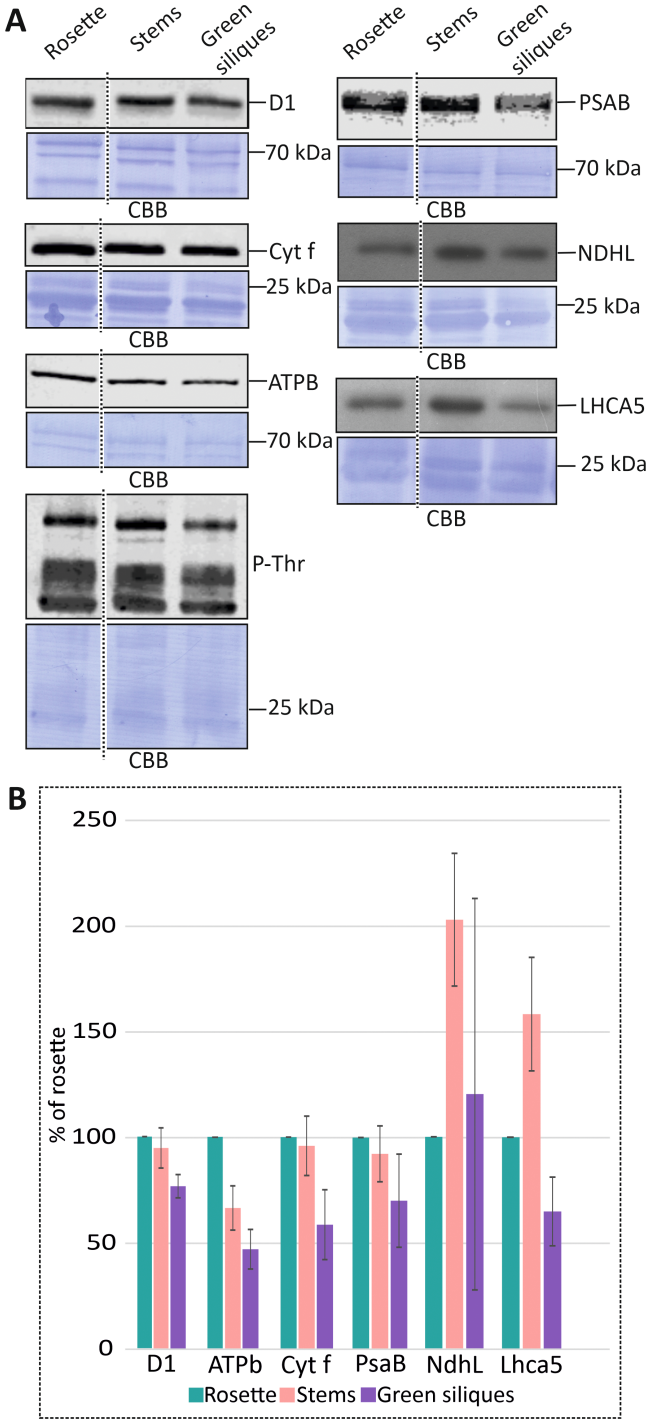

FIGURE 5 **Immunoanalysis of thylakoid proteins in distinct plant organs. (A)** Isolated thylakoid proteins from 5-week old rosettes, and 6-week old stems and green siliques (all WT) were analyzed on immunoblots using specific antibodies against D1, Cyt f, ATPB and PThr/Ser and PSAB, NDHL and LHCA5 proteins. Coomassie Brilliant Blue (CBB) staining was used to demonstrate even loading of the samples. (**B**) The quantification of immunoblots used to assess the amount of D1, Cyt f, ATPB, PSAB, NDHL and LHCA5 in thylakoid protein samples of rosettes, stems and green siliques (n = 3).

response to developmental stage of the plant. For instance, photosynthetic activity has been shown to be higher in young than in older leaves and to decrease gradually upon maturation both in Arabidopsis (Kitajima et al., 1997; Stessman et al., 2002) and in tobacco (Jiang & Rodermel, 1995). Previous studies have further shown that expression of several plastid-encoded genes related to photosynthesis are induced in young Arabidopsis tissues: a high amount of the *RbcL* transcripts (encoding the large subunit of Rubisco) and *psbA* transcripts (encoding the PSII core subunit D1) accumulates in young rosettes (Zoschke et al., 2007). ATPase subunit *atpB*, in contrast, shows only slight variation in leaves of different ages (Zoschke et al., 2007). It should be noted that in our study young and mature leaves represent the entire rosette containing leaves of different ages, and the expression pattern of an individual leaf (or cell type within the leaf) in a specific developmental stage may deviate from the results shown in Figure 2. Indeed, Berkowitz et al. (2021) have shown that although the amount of transcripts expressed in a single cell representing either mesophyll, epidermis or vasculature of Arabidopsis leaf is quite similar, significant proportion of genes appears to display unique expression patterns. Altogether, our results imply that it is essential to take the developmental stage of the plant into consideration when results from different studies are compared, or new experiments are planned.

4.2 | Plant organs show distinct expression patterns of photosynthetic genes

To our knowledge, a comprehensive comparison of the transcriptomic profiles of different plant organs with a focus on photosynthetic genes is currently lacking, even though important aspects of plant development and tissue specificity have been previously revealed through transcriptome analyses (Chen et al., 2021; Czechowski et al., 2004; Klepikova et al., 2016; Ma et al., 2005; Schmid et al., 2005). Our gene expression analysis showed that while the majority of genes are commonly expressed in all plant organs, they also possess a unique set of genes, which are expressed in one specific organ only (Figure S1A). The uniquely expressed genes in different organs, particularly in roots and flowers, were related to the specific functions of the organ, in line with a previous microarray analysis by Klepikova et al. 2016. Notably, green siliques were excluded from our RNA-Seq analysis due to poor success in RNA isolation, but a previous transcriptomic analysis has shown the expression of photosynthetic genes in green siliques (Mizzotti et al., 2018). Similarly to our results for ageing leaves (Figure 2B), expression levels of the photosynthetic genes showed a significant decrease upon maturation of the siliques (Mizzotti et al., 2018), which appears to be a universal trend in ageing green tissues.

Here, our focus was on the analysis of the expression of photosynthetic genes in different plant organs. In line with earlier studies (Klepikova et al., 2016; Schmid et al., 2005), we observed downregulation of photosynthesis-related genes in non-foliar organs (Figure 3). Further, few photosynthetic genes were upregulated in the non-foliar tissues as compared to leaves. The *TKL2* gene encoding an amphibolic enzyme involved in the plant carbon metabolism, taking part in both the CBB cycle and oxidative pentose phosphate (OPP) pathway (Villafranca & Axelrod, 1971) was heavily upregulated in all other

organs as compared to leaves. In the CBB cycle, TKL is a key player in the regenerative phase (Villafranca & Axelrod, 1971). OPP pathway is the main pathway for generating NADPH and other reductants in non-photosynthetic tissues, and the OPP pathway enzymes have been found in cytosol and plastids (Henkes et al., 2001). Arabidopsis contains two isoforms of *TKL*; *TKL1* (AT3G60750) and *TKL2* (AT2G45290), which are both located in chloroplasts (Kruger & Schaewen, 2003). Unlike *TKL2*, the *TKL1* isoform was downregulated in flowers, roots and stems (Figure 3). Our results are in line with previous studies suggesting that TKL1 is the key player in carbon allocation in leaves (Khozaei et al., 2015), and that TKL2 is the main isoform in non-foliar plant organs. In addition to *TKL2*, another photosynthesis-related gene, *ACHT1* was upregulated in non-foliar tissues, but the changes were statistically significant only in stems. ACHT1 is a chloroplast-located thioredoxin that accepts electrons from LET reactions and reduces 2-Cys-peroxiredoxin (Dangoor et al., 2012). 2-Cys-peroxiredoxin enzymes reduce peroxides and protect plants from oxidative stress (Dietz et al., 2002).

Other photosynthetic genes significantly upregulated in stems were *CP12-3*, *ACDO1* and *LHCB4.3*. CP12-3 mediates the formation of a complex that regulates CBB enzymes, glyceraldehyde 3-phosphate dehydrogenase (GAPDH) and phosphoribulokinase (PRK) (Marri et al., 2010). ACDO1, also known as PGR6, is a plastoglobulus-located atypical kinase reported to affect PQ homeostasis and adaptation to high light (Pralon et al., 2019; Yang et al., 2012). LHCB4.3, in turn, is part of the light-harvesting complex of PSII. *FBA3* and *PGK3* were significantly upregulated in flowers and in roots. In Arabidopsis, fructose 1,6-bisphosphate aldolase (FBA) is encoded by the *AtFBA1-AtFBA3* genes. FBA2 is the main isoform in leaves, while *FBA3* is mostly expressed in heterotrophic tissues (Carrera et al., 2021). Deficiency of FBA3 has an effect on leaf phloem transport and plastidial glycolytic metabolism of the root (Carrera et al., 2021). PGK (phosphoglycerate kinase) enzymes are also represented by three isoforms. PGK1 is exclusively located in chloroplasts of photosynthetic tissues, PGK2 in both photosynthetic and non-photosynthetic plastids, whereas PGK3 is in the cytosol of all tissue types (Rosa-Téllez et al., 2018). PGK3 takes part in glycolysis, gluconeogenesis and CBB cycle.

Even if the vast majority of the chloroplast targeted proteins are encoded in the nucleus, the central proteins of the photosynthetic machinery, e.g. the PSII core proteins D1 and D2, as well as the PSI core proteins PSAA and PSAB, are encoded by the plastid genome. It should be noted that in the present study, the method used for the production of the RNA-Seq library is based on polyA-enrichment. Although the chloroplast-encoded mRNAs are also polyadenylated, in plastids, the poly-A tail targets the transcripts for rapid degradation (Lange et al., 2009). Therefore, the chloroplast-encoded transcripts detected in our analysis do not represent the total pool of expressed chloroplast-encoded genes, and thus, the values cannot be used for reliable quantification. Future studies identifying expression patterns of plastid-encoded genes in distinct plant organs will complement the current dataset, and are likely to reveal interesting new features of non-foliar photosynthesis and plastid metabolism in general.

4.3 | Non-foliar plant organs possess leaf-type organization of thylakoid protein complexes with the exception of stems showing high accumulation of PSI-NDH

Although the expression of photosynthetic genes was downregulated in non-foliar organs, our non-denaturing BN-PAGE analysis of thylakoid protein complexes revealed that all necessary components of the photosynthetic electron transfer chain (PSII-LHCII, Cyt b_6f, PSI-LHCII and ATPase) were present in all studied organs (Figure 4). Accordingly, we did not observe marked differences in the abundance of specific photosynthetic proteins representing the main photosynthetic complexes PSII, Cyt b_6f, PSI and ATPase (D1, Cyt f, PSAB, ATPB, respectively) (Figure 5). Intriguingly, a high accumulation of PSI-NDH supercomplexes was observed in stems (Figure 4, Datasets S17-S21) (Kouril et al., 2014). The overall accumulation of PSI-NDH subunits LHCA5 and NDHL (Ifuru et al., 2011) in the thylakoid samples provided further evidence for the higher accumulation of the PSI-NDH complex in the stems (Figure 5).

These findings may indicate active CET through the PSI-NDH pathway, reflecting a higher demand for ATP in stems. Indeed, stems require ATP for the transportation of sugars and nutrients against a concentration gradient. In addition, phenylalanine is a precursor for lignin biosynthesis, and the generation of phenylalanine via the shikimate pathway requires ATP (Tohge et al., 2013; Vanholme et al., 2010). This could also explain the high demand for ATP in stems for the biosynthesis of phenylalanine, which is further metabolized into lignin. Genes involved in lignin biosynthesis, such as *PHENYLALANINE AMMONIA-LYASE 2* (AT3G53260), *CINNAMATE 4-HYDROXYLASE* (AT2G30490), *4-COUMARATE: COA LIGASE* (AT1G51680), *COUMARATE 3-HYDROXYLASE* (AT2G40890) and *HYDROXYCINNAMOYL-COA SHIKIMATE/QUINATE HYDROXYCINNAMOYL TRANSFERASE* (AT5G48930), were also significantly upregulated in stems (Dataset S10) further supporting the hypothesis that stems possess more active CET in order to fulfil the need for ATP.

Another intriguing curiosity is that the cells surrounding the vascular tissues of stems and petioles of C3 plants have been shown to resemble the bundle sheath cells of C4 plants (Hibberd & Quick, 2002; Kinsman & Pyke, 1998; Williams et al., 1989). These cells also possess characteristics of C4 photosynthesis, as they contain highly active forms of the key decarboxylases required for C4 photosynthesis (Hibberd & Quick, 2002). It was suggested that the photosynthetic cells surrounding the vascular system are supplied by inorganic carbon (malate or CO_2) from the xylem vessels, which is followed by decarboxylation of malate. Thereafter, the released CO_2 is used in photosynthesis to produce carbohydrates for the metabolism, growth and reproduction of plants (Hibberd & Quick, 2002). Intriguingly, in our analysis, one of the genes encoding a malic enzyme in Arabidopsis (AT2G19900, NADP-MALIC ENZYME 1) shows 7-fold upregulation in stems as compared to mature rosettes, and expression of the AT4G15530 gene encoding pyruvate orthophosphate dikinase is nearly 3-fold upregulated (Dataset S10). Although the sub-cellular localization of the enzymes has not been confirmed yet, it is tempting

to speculate that the C4-type photosynthesis could also take place in the stems of Arabidopsis, similarly to those of tobacco (Hibberd & Quick, 2002). Further research is needed to provide a detailed role of CET in the stems of C3 plants.

AUTHOR CONTRIBUTIONS

P.M., E.T. and M.R. designed the research: L.L, M.R. and U.R. performed the research; L.L., M.R., P.M. and E.T. analyzed the data; L.L. wrote the paper with contributions from P.M., M.R. and E.T.

ACKNOWLEDGEMENTS

We thank Tapio Lempiäinen and Juha Kurkela for their generous advice and Maisa Pikkarainen and Tiia Siivola for technical assistance. RNA-Seq analyses were performed at the Finnish Functional Genomics Centre supported by the University of Turku, Åbo Akademi University and Biocenter Finland, and mass spectrometry analyses at the Turku Proteomics Facility supported by Biocenter Finland. Finnish Infrastructure for Photosynthesis Research PHOTOSYN is acknowledged for the excellent research facilities. This study was supported by the Academy of Finland (321616 for LL, MR, UR and PM, 333421 for ET) and the Finnish Cultural Foundation (00220578 Keskusrahasto for LL, 00230972 for MR).

FUNDING INFORMATION

Academy of Finland (321616 for LL, MR, UR and PM, 333421 for ET); The Finnish Cultural Foundation (00220578 Keskusrahasto for LL, 00230972 for MR).

DATA AVAILABILITY STATEMENT

RNA-Seq data are available in GEO, accession GSE233562 https://www.ncbi.nlm.nih.gov/geo/info/linking.html.

ORCID

Laura Laihonen https://orcid.org/0000-0002-9243-7028
Marjaana Rantala https://orcid.org/0000-0002-2233-3805
Esa Tyystjärvi https://orcid.org/0000-0001-6808-7470
Paula Mulo https://orcid.org/0000-0002-8728-3204

REFERENCES

Albanese, P., Nield, J., Tabares, J. A., Chiodoni, A., Manfredi, M., Gosetti, F., Marengo, E., Saracco, G., Barber, J., & Pagliano, C. (2016) Isolation of novel PSII-LHCII megacomplexes from pea plants characterized by a combination of proteomics and electron microscopy. *Photosynthesis Research*, 130, 19–31.

Aro, E-M., Suorsa, M., Rokka, A., Allahverdiyeva, Y., Paakkarinen, V., Saleem, A., Battchikova, N. & Rintamäki, E. (2005) Dynamics of photosystem II: a proteomic approach to thylakoid protein complexes. *Journal of Experimental Botany*, 56, 347–356.

Aro, E-M., Virgin, I. & Andersson, B. (1993) Photoinhibition of photosystem II. Inactivation, protein damage and turnover. *Biochimica et Biophysica Acta*, 1143, 113–134.

Baumgartner, B.J., Rapp, J.C. & Mullet, J.E. (1989) Plastid transcription activity and DNA copy number increase early in barley chloroplast development. *Plant Physiology*, 89, 1011–1018.

Berkowitz, O., Xu, Y., Liew, L. C., Wang, Y., Zhu, Y., Hurgobin, B., Lewsey, M. G., & Whelan, J. (2021) RNA-seq analysis of laser microdissected *Arabidopsis thaliana* leaf epidermis, mesophyll and vasculature defines tissue-specific transcriptional responses to multiple stress treatments. *The Plant Journal*, 107, 938–955.

Blum, H., Beier, H. & Gross, H.J. (1987) Improved silver staining of plant proteins, RNA and DNA in polyacrylamide gels. *Electrophoresis*, 8, 93–99.

Carrera, D.Á., George, G.M., Fischer-Stettler, M., Galbier, F., Eicke, S., Truernit, E., Streb, S., & Zeeman, S. C. (2021) Distinct plastid fructose bisphosphate aldolases function in photosynthetic and non-photosynthetic metabolism in Arabidopsis. *Journal of Experimental Botany*, 72, 3739–3755.

Chen, S., Xu, X., Ma, Z., Liu, J. & Zhang, B. (2021) Organ-Specific Transcriptome Analysis Identifies Candidate Genes Involved in the Stem Specialization of Bermudagrass (*Cynodon dactylon* L.). *Frontiers in Genetics*, 12:678673.

Czechowski, T., Bari, R.P., Stitt, M., Scheible, W.R. & Udvardi, M.K. (2004) Real-time RT-PCR profiling of over 1400 Arabidopsis transcription factors: unprecedented sensitivity reveals novel root- and shoot-specific genes. *The Plant Journal*, 38, 366–379.

Dangoor, I., Peled-Zehavi, H., Wittenberg, G., & Danon, A. (2012) A chloroplast light-regulated oxidative sensor for moderate light intensity in Arabidopsis. *The Plant Cell*, 24, 1894–1906.

Dietz, K.J., Horling, F., König, J. & Baier, M. (2002) The function of the chloroplast 2-cysteine peroxiredoxin in peroxide detoxification and its regulation. *Journal of Experimental Botany*, 53, 1321–1329.

Henkes, S., Sonnewald, U., Badur, R., Flachmann, R. & Stitt, M. (2001) A small decrease of plastid transketolase activity in antisense tobacco transformants has dramatic effects on photosynthesis and phenylpropanoid metabolism. *The Plant Cell*, 13, 535–551.

Henry, R. J., Furtado, A., & Rangan, P. (2020) Pathways of photosynthesis in non-leaf tissues. *Biology*, 9, 438.

Hibberd, J.M. & Quick, W.P. (2002) Characteristics of C-4 photosynthesis in stems and petioles of C-3 flowering plants. *Nature*, 415, 451–454.

Jiang, C.Z. & Rodermel, S.R. (1995) Regulation of photosynthesis during leaf development in RbcS antisense DNA mutants of tobacco. *Plant Physiology*, 107, 215–224.

Johnson G.N. (2011) Physiology of PSI cyclic electron transport in higher plants. *Biochimica et Biophysica Acta*, 1807, 384–389.

Järvi, S., Suorsa, M., Paakkarinen, V. & Aro, E-M. (2011) Optimized native gel systems for separation of thylakoid protein complexes: novel super- and mega-complexes. *Biochemical Journal*, 439, 207–214.

Kallio, M.A., Tuimala, J.T., Hupponen, T., Klemelä, P., Gentile, M., Scheinin, I., Koski, M. Käki, J. & Korpelainen, E.I. (2011) Chipster: user-friendly analysis software for microarray and other high-throughput data. *BMC Genomics*, 12, 507.

Khozaei, M., Fisk, S., Lawson, T., Gibon, Y., Sulpice, R., Stitt, M., Lefebvre, S. C., & Raines, C. A. (2015) Overexpression of plastid transketolase in tobacco results in a thiamine auxotrophic phenotype. *The Plant Cell*, 27, 432–447.

Kinsman, E.A. & Pyke, K.A. (1998) Bundle sheath cells and cell-specific plastid development in Arabidopsis leaves. *Development*, 125, 1815–1822.

Kitajima, K., Mulkey, S., & Wright, S. (1997) Decline of photosynthetic capacity with leaf age in relation to leaf longevities for five tropical canopy tree species. *American Journal of Botany*, 84, 702.

Klepikova, A.V., Kasianov, A.S., Gerasimov, E.S., Logacheva, M.D. & Penin, A.A. (2016) A high resolution map of the Arabidopsis thaliana developmental transcriptome based on RNA-seq profiling. *The Plant Journal*, 88, 1058–1070.

Kong, L., Wang, F., Feng, B., Li, S., Si, J. & Zhang, B. (2010) The structural and photosynthetic characteristics of the exposed peduncle of wheat (*Triticum aestivum L.*): an important photosynthate source for grain-filling. *BMC Plant Biology*, 10, 1–10.

Kouřil, R., Strouhal, O., Nosek, L., Lenobel, R., Chamrád, I., Boekema, E. J., Šebela, M., & Ilík, P. (2014) Structural characterization of a plant

photosystem I and NAD(P)H dehydrogenase supercomplex. *The Plant Journal*, 77, 568–576.
Kruger, N. J., & von Schaewen, A. (2003) The oxidative pentose phosphate pathway: structure and organisation. *Current Opinion in Plant Biology*, 6, 236–246.
Lange, H., Sement, F.M., Canaday, J. & Gagliardi, D. (2009) Polyadenylation-assisted RNA degradation processes in plants. *Trends in Plant Science*, 14, 497–504.
Langmead, B., & Salzberg, S.L. (2012) Fast gapped-read alignment with Bowtie2. *Nature Methods*, 9, 357–360.
Love, M.I., Huber, W., & Anders, S. (2014) Moderated estimation of fold change and dispersion for RNA-seq data with DESeq2. *Genome Biology*, 15, 550.
Ma, L., Sun, N., Liu, X., Jiao, Y., Zhao, H. & Deng, X.W. (2005) Organ-specific expression of Arabidopsis genome during development. *Plant Physiology*, 138, 80–91.
Marri, L., Pesaresi, A., Valerio, C., Lamba, D., Pupillo, P., Trost, P., & Sparla, F. (2010) In vitro characterization of Arabidopsis CP12 isoforms reveals common biochemical and molecular properties. *Journal of Plant Physiology*, 167, 939–950.
Mizzotti, C., Rotasperti, L., Moretto, M., Tadini, L., Resentini, F., Galliani, B.M, Galbiati, M., Engelen, K., Pesaresi, P. & Masiero, S. (2018) Time-course transcriptome analysis of Arabidopsis siliques discloses genes essential for fruit development and maturation. *Plant Physiology*, 178, 1249–1268.
Munekage, Y., Hashimoto, M., Miyake, C., Tomizawa, K., Endo, T., Tasaka, M., & Shikanai, T. (2004) Cyclic electron flow around photosystem I is essential for photosynthesis. *Nature*, 429, 579–582.
Munné-Bosch, S. & Alegre L. (2002) Plant aging increases oxidative stress in chloroplasts. *Planta*, 214, 608–615.
Müller, P., Li, X.P. & Niyogi K.K. (2001) Non-photochemical quenching. A response to excess light energy. *Plant Physiology*, 125, 1558–1566.
Otani, T., Kato, Y., & Shikanai, T. (2018) Specific substitutions of light-harvesting complex I proteins associated with photosystem I are required for supercomplex formation with chloroplast NADH dehydrogenase-like complex. *The Plant Journal*, 94, 122–130.
Porra, R.J., Thompson, W.A. & Kriedmann, P.E. (1989) Determination of accurate extinction coefficients and simultaneous equations for assaying chlorophylls a and b extracted with four different solvents: verification of the concentration of chlorophyll standards by atomic absorption spectroscopy. *Biochimica et Biophysica Acta*, 975, 384–394.
Pralon, T., Shanmugabalaji, V., Longoni, P., Glauser, G., Ksas, B., Collombat, J., Desmeules, S., Havaux, M., Finazzi, G., & Kessler, F. (2019) Plastoquinone homoeostasis by Arabidopsis proton gradient regulation 6 is essential for photosynthetic efficiency. *Communications Biology*, 2, 220.
Putri, G.H., Anders, S., Pyl, P.T., Pimanda, J.E., & Zanini, F. (2022) Analysing high-throughput sequencing data in Python with HTSeq 2.0. *Bioinformatics*, 38, 2943–2945.
Rosa-Téllez, S., Anoman, A. D., Flores-Tornero, M., Toujani, W., Alseek, S., Fernie, A. R., Nebauer, S. G., Muñoz-Bertomeu, J., Segura, J., & Ros, R. (2018) Phosphoglycerate kinases are co-regulated to adjust metabolism and to optimize growth. *Plant Physiology*, 176, 1182–1198.
Sánchez-Díaz, M., García, J., Antolín, M. & Araus, J.L. (2002) Effects of soil drought and atmospheric humidity on yield, gas exchange, and stable carbon isotope composition. *Photosynthetica*, 40, 415–421.
Saveyn, A., Steppe, K., Ubierna, N. & Dawson, T.E. (2010) Woody tissue photosynthesis and its contribution to trunk growth and bud development in young plants. *Plant, Cell and Environment*, 33, 1949–1958.
Schmid, M., Davison, T.S., Henz, S.R., Pape, U.J., Demar, M., Vingron, M., Schölkopf, B. & Weigel, D. (2005) A gene expression map of *Arabidopsis thaliana* development. *Nature Genetics*, 37, 501–506.
Shikanai, T. (2007) Cyclic electron transport around photosystem I: Genetic approaches. *Annual Review of Plant Biology*, 58, 199–217.
Shimizu, H., Peng, L., Myouga, F., Motohashi, R., Shinozaki, K., & Shikanai, T. (2008) CRR23/NdhL is a subunit of the chloroplast NAD(P)H dehydrogenase complex in Arabidopsis. *Plant and Cell Physiology*, 49, 835–842.
Simkin, A. J., Faralli, M., Ramamoorthy, S., & Lawson, T. (2020) Photosynthesis in non-foliar tissues: implications for yield. *The Plant Journal*, 101, 1001–1015.
Stessman, D., Miller, A., Spalding, M., & Rodermel, S. (2002). Regulation of photosynthesis during Arabidopsis leaf development in continuous light. *Photosynthesis Research*, 72, 27–37.
Sun, W., Ma, N., Huang, H., Wei, J., Ma, S., Liu, H., Zhang, S., Zhang, Z., Sui, X. & Li, X. (2021) Photosynthetic contribution and characteristics of cucumber stems and petioles. *BMC Plant Biology*, 21, 454.
Tiwari, A., Mamedov, F., Grieco, M., Suorsa, M., Jajoo, A., Styring, S., Tikkanen, M. & Aro, E.M. (2016) Photodamage of iron–sulphur clusters in photosystem I induces non-photochemical energy dissipation. *Nature Plants*, 2, 16035.
Tohge, T., Watanabe, M., Hoefgen, R. & Fernie, A. (2013) Shikimate and phenylalanine biosynthesis in the green lineage. *Frontiers in Plant Science*, 4, 62.
Vanholme, R., Demedts, B., Morreel, K., Ralph, J. & Boerjan, W. (2010) Lignin biosynthesis and structure. *Plant Physiology*, 153, 895–905.
Villafranca, J.J. & Axelrod, B. (1971) Heptulose synthesis from nonphosphorylated aldoses and ketoses by spinach transketolase. *Journal of Biological Chemistry*, 246, 3126–3131.
Williams, M.L., Farrar, J.F. & Pollock, C.J. (1989) Cell specialization within the parenchymatous bundle sheath of barley. *Plant, Cell & Environment*, 12, 909–918.
Xu, H.-L., Gauthier, L., Desjardins, Y., & Gosselin, A. (1997) Photosynthesis in leaves, fruits, stem and petioles of greenhouse-grown tomato plants. *Photosynthetica*, 33, 113–123.
Yang, S., Zeng, X., Li, T., Liu, M., Zhang, S., Gao, S., Wang, Y., Peng, C., Li, L. & Yang, C. (2012) AtACDO1, an ABC1-like kinase gene, is involved in chlorophyll degradation and the response to photooxidative stress in Arabidopsis. *Journal of Experimental Botany*, 63, 3959–3973.
Yiotis, C., Psaras, G.K. & Manetas, Y. (2008) Seasonal photosynthetic changes in the green-stemmed Mediterranean shrub *Calicotome villosa*: A comparison with leaves. *Photosynthetica*, 46, 262–267.
Zoschke, R., Liere, K. & Börner, T. (2007) From seedling to mature plant: Arabidopsis plastidial genome copy number, RNA accumulation and transcription are differentially regulated during leaf development. *The Plant Journal*, 50, 710–722.

SUPPORTING INFORMATION

Additional supporting information can be found online in the Supporting Information section at the end of this article.

How to cite this article: Laihonen, L., Rantala, M., Ranasinghe, U., Tyystjärvi, E. & Mulo, P. (2024) Transcriptomic and proteomic analyses of distinct Arabidopsis organs reveal high PSI-NDH complex accumulation in stems. *Physiologia Plantarum*, 176(2), e14227. Available from: https://doi.org/10.1111/ppl.14227